VERTICAL BIOMASS DISTRIBUTION DRIVES FLOW THROUGH AQUATIC VEGETATION

Raúl Villanueva[1,*], Maike Paul[2], Miriam Vogt[1] and Torsten Schlurmann[1]

Abstract: Seagrass meadows represent important ecosystems providing many services, which have been disappearing, mostly due to anthropogenic reasons. Restoration attempts require deep understanding of the hydrodynamics involved, as well as the role of the biomechanical traits of the plants. This study analyzes the utilization of artificial elements as seagrass surrogates and their effect on flow. The surrogates are tested against a unidirectional current in a circular track-flume at velocities of 5, 10, 20 and 30 cm/s for three different vertical biomass distributions to assess the influence of biomechanical traits. Results show that the vertical biomass distribution plays an important role in the reduction of current velocity. The low shoot density tested also proved to be enough to onset current reduction utilizing artificial elements. This proves that ecosystem services such as sedimentation and energy dissipation are reproducible with artificial elements, and can be used as means for restoration and protection.

INTRODUCTION

Coastal zones around the globe are becoming a focus point on research due to the strong linkage with human livelihood. With an increasing ratio of the population living near coastlines, the focus point for human safety shifts towards a sustainable human-environment interaction. This encompasses an efficient use of resources for food, geography for transport and the coastal environment for protection. Coastal protection has been an area of focus on the past couple centuries, where the paradigm was the implementation of hard engineering; however, these structures change the environment and ecosystems drastically (Orth et al., 2006), taking a great toll on coastal ecosystems. Restoration and preservation of these ecosystems is important for the environment and for human safety, and recent studies on this importance have led to a special interest on the role of these ecosystems on coastal protection. This way they have come forward on the scene of Ecological Solutions for Disaster Risk Reduction (Eco-DRR, as mentioned in the Sendai Framework for Disaster Risk Reduction, SFDRR, UNISDR, 2015).

Within the framework of the project *SeaArt: Long-term establishment of seagrass ecosystems through artificial biodegradable meadows*, the role of seagrasses on coastal hydrodynamics is investigated. With seagrass ecosystem services in mind, the project aims towards seagrass restoration. Seagrass meadows worldwide have retreated drastically in the past decades (Waycott et al., 2009); furthermore, restoration attempts have been emerging recently with a range of methodologies being tested, but success rate still very low (see e.g. Van Katwijk et al., 2009; Peralte et al.,

[1] Leibniz Universität Hannover, Ludwig-Franzius Institute for Hydraulic, Estuarine and Coastal Engineering. Nienburger Str. 4, 30167 Hanover, Germany. Emails: *villanueva@lufi.uni-hannover.de; vogt@lufi.uni-hannover.de; schlurmannvogt@lufi.uni-hannover.de
[2] Technische Universität Braunschweig, Institute of Geoecology, Department of Lanscape Ecology and Environmental System Analysis. Langer Kamp 19c, 38106 Brunswick, Germany. Email: m.paul@tu-braunschweig.de

2003; Tuya et al., 2017). As a countermeasure, the project proposes the use of biodegradable artificial elements in order to create an onset for seagrass growth. This would be achieved through energy dissipation in the form of reduced current velocity and wave loads, thus increasing sedimentation and consequently aiding seagrass seeds settle and grow.

To achieve this goal, the interaction between seagrass and its surrounding aquatic environment needs to be well understood. The artificial seagrass (ASG), or surrogates, should be able to resist the hydrodynamic loadings the same way seagrass meadows do so to protect themselves – and even in a greater scale – in order to achieve long-term protection for seedlings. Studies on vegetation and hydrodynamics have flourished in recent years, with plenty of experimental set-ups being tested for vegetation and corresponding loadings (e.g. Gambi et al., 1990; Bouma et al., 2005; Paul & Gillis, 2015; Paul et al., 2016; Möller et al., 2014). Moreover, within the context of *SeaArt*, we aim to broaden the current understanding of vegetated hydrodynamics by including the surrogates in order to obtain suitable (artificial) meadow characteristics whose presence enhances seagrass resettlement. The first step is then to understand the underlying current-structure interaction, whereby processes are complex due to the flexible characteristics of the structure with strong implication on the surrounding flow field. This is done through physical experiments in a circular track-flume, where the surrogates are loaded with a one-directional current at different velocities. The methodology section in this paper explains more in detail the procedure done during experimentation; but first, a clear understanding of (1) the role of seagrass in the coastal ecosystem in terms of ecology as well as coastal hydrodynamics and (2) the active forces present and the fluid-structure interaction, is needed, which is outlined in the following section.

SEAGRASS WITHIN THE COASTAL ECOSYSTEM

The area of study is set to be the north German coast and the focus species *Zostera marina,* one of the four major seagrass species in Europe (Ondiviela et al., 2014), present in both the North and Baltic seas. Fig. 1 shows examples of the focus species in the German North and Baltic Sea.
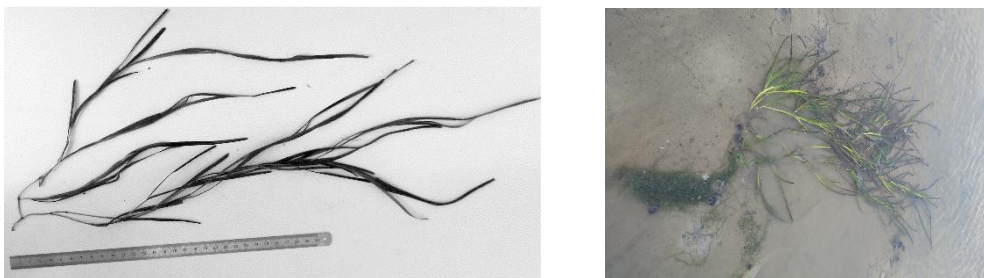

Figure 1. *Z. marina* examples from the Baltic Sea (left) and North Sea (Right).

Seagrasses reduce current velocities, as well as wave heights, within the surf zone (Koch et al., 2007; Paul et al., 2012). This in turn increases sedimentation, which lowers turbidity and increases light availability within the meadows. Causal relations and implications are an adaptation mechanism developed by seagrasses and other aquatic vegetation in order to ensure maximum light uptake and a stable ground (Koch, 2001). The very flexibility of seagrasses is another survival mechanism, where

the structural reconfiguration serves the purpose of minimization of hydrodynamic loading (Luhar & Nepf, 2011), hence providing ideal conditions for growth. Just as other aquatic vegetation, seagrasses adapt by reducing hydrodynamic loading in order to allow sedimentation; additionally, they also adapt to the velocity by streamlining in order to (1) reduce the hydrodynamic loading, thus not being ripped off their roots, and (2) stimulate pollenization (Koch et al., 2006; Gambi et al., 1990).

Understanding the processes and driving forces that lead to structural reconfiguration and consequent energy dissipation is of vital importance for the evaluation of the system as a whole as a soft measure of coastal protection. Moreover, the conditions needed for adequate plant growth and survival also eventuate from these processes.

Active Forces

In order to mimic the demanded conditions for growth, forces acting on the plants and surrogates are studied through physical experiments under controlled conditions. Here, we focus on a unidirectional current using polyethylene surrogates with the characteristics shown later in Table 1. These surrogates, like actual seagrasses, are exposed to currents which exert a force on each individual element. This is the drag force, which is the consequence of inertial and viscous forces acting on the element by the moving fluid (Vogel, 1994). The surrogates, in exchange, exert a resistance which can be directly related to the buoyancy and flexural rigidity of the element (Niklas, 1992; Fonseca & Koehl, 2006).

These forces have been thoroughly studied and represented in physical and analytical models (see e.g. Nepf & Vivoni, 2000; Ghisalberti & Nepf, 2009; Losada et al., 2016) regarding the effects of vegetation, both artificial and natural, on coastal hydrodynamics. Each study proves how a form-specific vegetative element reduces current and orbital velocities and creates a dampening effect on waves and currents, whereby plant biomechanical properties and drag play an important role. This study, however, focuses on assessing the effect of vertical biomass distribution (VBD) on hydrodynamics and the effectiveness of surrogates to mimic actual seagrasses. The next section explains in detail the characteristics of the elements used, whereby an idealized set-up was built by varying the VBD used on the meadows, but maintaining biomechanical and spatial parameters constant. This means that buoyant and drag forces within the meadow will vary according to the vertical distribution of biomass, but not depending on the total biomass of the meadow.

METHODOLOGY

The effect of ASG resembling *Z. marina* is investigated against a unidirectional current in a circular track-flume. The flume is part of the facilities of the Ludwig-Franzius-Institute for Hydraulic, Estuarine and Coastal Engineering in Hanover, Germany; it has a width of 1 m and maximum water level of 60 cm (for detailed information about the flume, see Goseberg et al., 2013; Schendel et al., 2015). Our experiments test the ASG effects against low-range currents (i.e. 0.05, 0.1, 0.2 and 0.3 m/s). This allows for a preliminary assessment of (1) the ability of the chosen ASG to resist commonly found currents on coastal ecosystems, and (2) its suitability to mimic the ecosystem service of actual seagrass by dampening current velocity.

As a surrogate for the focus seagrass, *Z. marina*, polyethylene band (commonly known as gift ribbon) with a density of 0.45 g/cm^3 was used. As in other studies (e.g.

Villanueva, Paul, Vogt and Schlurmann

Bouma et al., 2005; Paul et al., 2016; Tuya et al., 2017), polyethylene has proven a suitable surrogate for experimentation due to its similar buoyant nature with respect to seagrasses. Furthermore, the ASG meadows should be able not only to mimic actual seagrass, but allow for light penetration and simultaneous sedimentation within the meadow. In order to achieve both objectives, a balanced shoot density within the meadow is needed. For this, a specific shoot density was chosen in order to investigate current reduction capacities of an ASG meadow whose density lies in the lower limits of usual nature-found densities of *Z. marina* patches. The size of the individual blades was selected with a similar criterion in mind. Ondiviela et al. (2014) have a thorough review of seagrass meadow parameters, including *Z. marina*, which served as base for the selection of shoot density, leaf (or blade) length and width of the ASG (see table 1). Moreover, the shoot density can be described by the roughness density, as described by Nepf (2012).

$$\lambda_f = \int_{z=0}^{h} a dz = ah \qquad (1)$$

where λ_f (or ah) is the roughness density, a defines the frontal area per canopy volume and h is the canopy height – also referred to as effective canopy height – representing the average height of the canopy after bending through current load.

Additionally, the experiments also sought to investigate the effects vertical biomass distribution (VBD) on current reduction. In order to obtain comparable results regarding VBD, it was the only parameter that varied between experiments – i.e. shoot density, total biomass and blade length were kept constant, while the distribution of biomass within a shoot was set to 3 variations: (a) biomass uniformly distributed along the length of the blades in each shoot, thus having constant width; (b) biomass concentrated in the upper half of the shoot and (c) biomass concentrated on the lower half (Table 1 and Figure 2).

Table 1 ASG parameters chosen for the different VBDs tested.

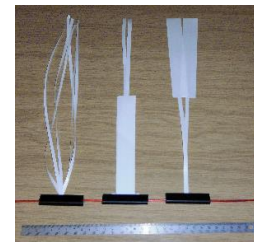| shoot density [shoots/m2]	Biomass concentration	Blade length [cm]	Number of blades	width up [mm]	width down [mm]
105	Constant	30	6	5	5
	Upper part		2	25	5
	Lower part		2	5	25

Figure 2 Different VBDs tested

The VBDs selected for this study could be easily related to different coastal vegetation found in nature, e.g. seaweed *Fucus serratus* and cord-grass *Spartina anglica* whose biomechanical composition comprises high biomass concentration on the upper and lower parts of the plant, respectively (Paul et al., 2014; Bouma et al., 2005). A constant VBD, in turn, assimilates *Z. marina*. This helps assess the role of VBD on current reduction, and how different seagrass species affect the flow. It is worth noting, however, that these experiments depict an idealized case where all surrogates have the same mechanical properties, whereas the actual seagrasses mentioned would have very different biomechanical features. The differences in VBD

4

cause differences in the flexural stiffness (or bending rigidity), which, in simple terms, can be given by *EI,* where *E* is the Young's Modulus and *I* is the second moment of inertia. The latter term is given (for a rectangular shape) by $(1/12)bh^3$, suggesting that an increase in *h*, which is parallel to the flow in the cross-sectional direction, is exponentially more significant than increasing the width *b* (perpendicular to the flow). Our experiments, however, only vary the width, thus affecting the roughness density (*ah*) more than the flexural stiffness.

Experimental Set-up

The selected ASG dimensioning (different VBDs) was set up in the aforementioned flume in two 1-by-1-m patches, as shown in figure 3. This allowed for an assessment of the role of meadow length (*x*) on attenuation; nevertheless, flume size, time and reach of the instrument-ready section of the flume did not allow for more than two patches in total. The patches were separated from each other by 40 cm, which allowed for an unobstructed measurement point behind the first ASG patch. The shoots were placed within 10 cm of each other in the *x* and *y*-direction, alternating each subsequent row with a displacement of 5 cm with respect to the preceding row in the *y*-direction (figure 3b). This was done to avoid a formation of streams within the meadows through each 10-cm gap between shoots, thus optimizing shoot frontal cover against the flow for the chosen density, while at the same time adding a little bit of randomness to assimilate nature.
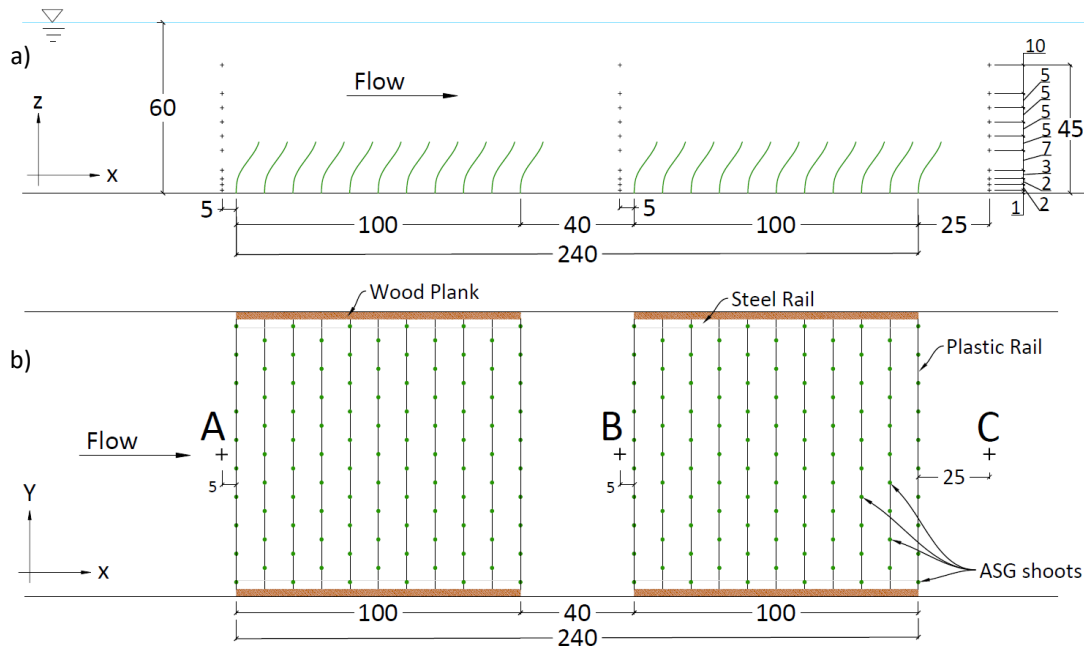

Figure 3 Experimental set-up used in the race track-flume, (a) side view and (b) top view**.** + mark the measurement points in the *z* and *x*- directions. All units in mm.

Each VBD was tested against mean velocities of 5, 10, 20 and 30 cm/s constant through the measuring timespan. These mean velocities were first measured in a homogeneous flow field without the presence of ASG, from now on referred to as "reference case", and were measured at 3 different points: A, B and C (see figure 3), thus forming 3 profiles. Profile A was 5 cm in front of the first meadow; B was 5 cm

5

in front of the second meadow, hence 35 cm behind the first meadow; and C was 25 cm behind the second meadow. This gave a total sample distance of 2.70 m, between A and C. Each obtained velocity profile consisted of 10 measurement points with a finer resolution at the bottom, as shown in figure 3a. The total water height used was $H = 0.60\ m$ measured during still water conditions.

Instrumentation

Current velocity was obtained utilizing a Nortek AS® Vectrino+ Acoustic Doppler Velocimeter (ADV) at a 25-Hz sampling frequency at each point marked by a + (plus sign) in figure 3a. The ADV was mounted on an automated process controller, which is itself mounted atop the walls of the flume and is movable along 3m in the *x*-direction. This allowed for measurements among the two 1x1-m plots. The process controller was programmed to lead the ADV to the center of the channel (*y*-direction) and carry out the measurements at each point. The ADV measured for a period of 1 min at each point, before moving to the next one, thus providing the velocity profiles at A, B and C, which are described in the next section.

The data from the ADV was processed using a low-pass filter with a 30% cut-off frequency. Additionally, a "despiking filter" based on the acceleration method described by Goring & Nikora (2002) was used to remove unwanted extremes during the measurements, especially near the bed, where values can be greatly affected by signal echoing on the floor, causing a very noisy output. The filter was applied to every coordinate individually with correlation and sound-to-noise ratio (SNR) as filter criteria. The *x*-direction took priority with the highest criteria used, ranging between 80-90% of correlation and $SNR > 15\ db$. The *y* and *z*-directions had regularly less stern limits.

Finally, Logitech® C920 HD-cameras were used to capture the movement of the ASG under the different currents. The flume features a 3-m window for model observation, which allowed for recording of the bending angles of the ASG through the use of a transparent raster (1x1cm resolution). At least 10 measurements for each velocity were recorded and averaged in order to obtain an idealized stable plant position under the given velocity by removing fluctuations caused by swaying. This, however, is only conceptual, and swaying should be always considered as it is an important factor in turbulence and vortex formation (Okamoto et al., 2016).

RESULTS

Initial analysis of the data appears to be in line with studies involving either natural or artificial vegetation (e.g. Nepf, 2012; Koch et al., 2006; Okamoto et al., 2016; Nepf & Vivoni, 2000), where a clear transition can be seen in the velocity profile in the above-canopy layer for completely submerged vegetation – clearly visible in the velocity profiles in figure 4. This shows how the velocity is significantly lower within the canopy; when compared to the reference case, the above-canopy water column showed a slight increase in velocity. This phenomenon has also been documented in some of the physical experiments cited above, which can be simply explained by the relative reduction in water column as well as velocity reduction caused by the presence of seagrass (here ASG) in the lower layer. This, in turn, produces an inflection point above the canopy where a shear-like layer can be observed; this layer marks the effect that the canopy has on flow, and for unidirectional flows, like in this case, it has been quantified depending on the canopy density (Nepf, 2012). The chosen
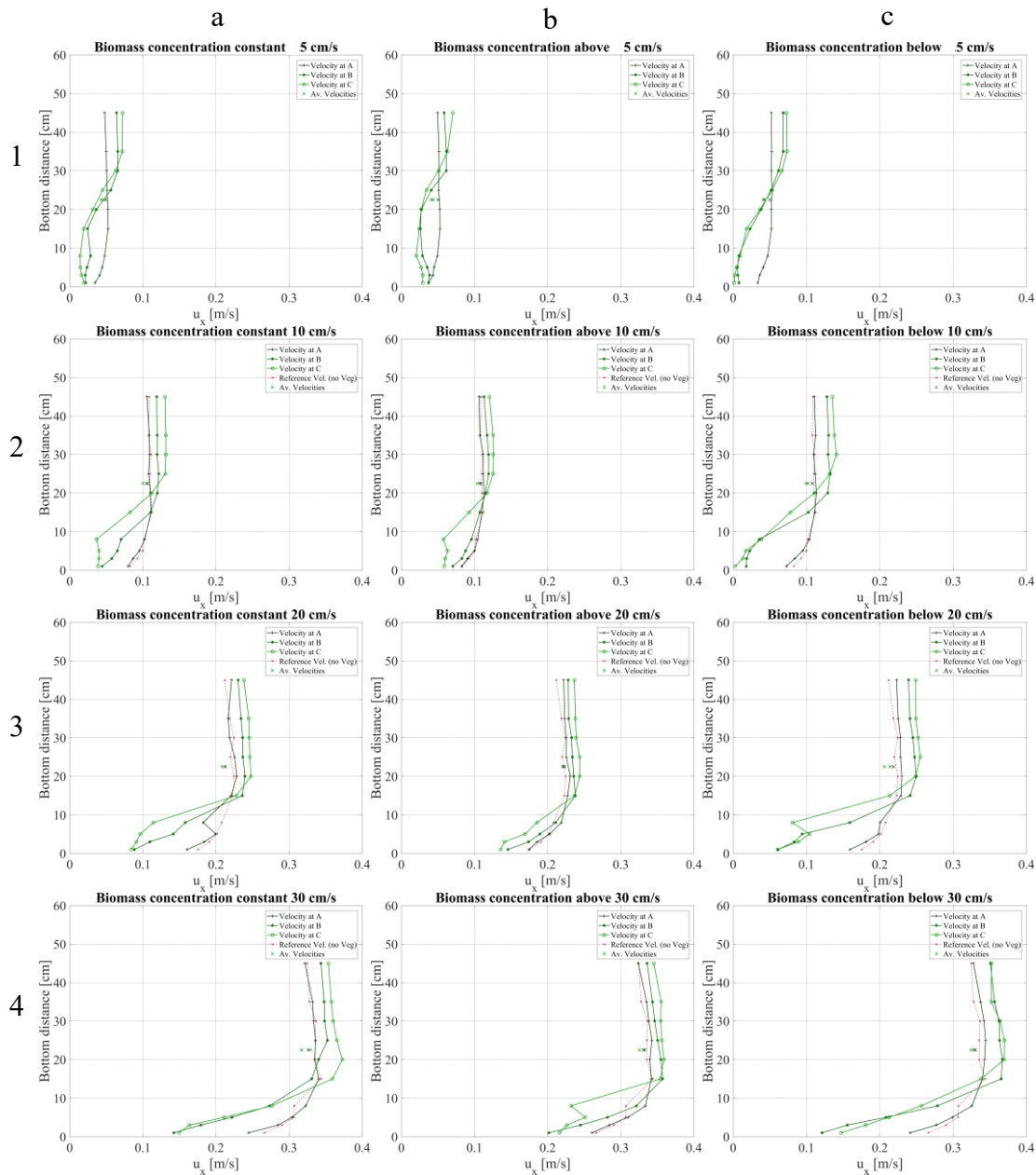
Villanueva, Paul, Vogt and Schlurmann

Figure 4 Velocity profiles at each measuring point – A, B and C– for each VBD: (a) *constant*, (b) *above* and (c) *below*; and each mean velocity: (1) 5 cm/s, (2) 10 cm/s, (3) 20 cm/s and (4) 30 cm/s.

shoot density falls into the classification: *transitional*, described by Belcher et al. (2003) – as cited and explained by Nepf, (2012) – for a roughness density $ah\sim0.1$. This marks the onset of the distorted profiles created by the canopy drag, meaning that drag within the canopy, and not bed roughness, represents the driving factor for velocity reduction (Nepf, 2012). Fig. 4 presents an array of plots, each of which shows the different velocity profiles measured with the ADV at points A, B and C, therefore representing how the profile changed in *x* for a given constant velocity. Columns a, b and c show the comparison of velocity profiles for each VBD: *constant*, *above* and *below*, respectively; whereas rows 1-4 present the velocity setting used: 5-30 cm/s. Additionally, the pink profile represents a comparison with the reference case.

Following the goal of restoration, the selected shoot density is relatively low in order to allow for light penetration and space for plant growth. This means that the

roughness density is quite low. Within the velocity profiles shown in Figure 4, the reduction in velocity is clear at the start of the canopy layer. The flexible character of the ASG makes its effective height, *h,* lower than the full length of the blades (30 cm), hence the initiation of reduction between 12 and 20 cm, depending on the velocity. All profiles show at least a slight reduction in velocity; however, the behavior of the profile changes. Velocity profiles at B and C for $u_x = 30 \, cm/s$ show a reduction for all VBDs, nevertheless the profile shape resembles that of the reference measurement, meaning there is only element-scale turbulence present; then bed drag – with some small contribution from vegetation drag – works as boundary layer (Nepf, 2012). The same can be said for the profiles with $u_x = 20 \, cm/s$ at B and C for VBDs *above* and *below* and at B for VBD *constant*. Profile C for VBD *constant*, on the other hand (as well as all profiles at C for all VBDs at lower velocities), show something different: the inflection point is present and the profile now has an S-shaped form created by the shear-like layer at the top of the canopy. For lower velocities, effective height, *h*, is close to the actual height of 30 cm; we obtain thence a roughness density nearer 0.1 (e.g. $ah = 0.09$ for 5-mm blades at 10-cm spacing, 30-cm height and *constant* VBD), where – in accordance to Belcher et al., (2003) – the transitional condition, hence the inflection point, occur. Conversely, calculation of *ah* for a 10-cm separation and 25-mm blade width yields values up to 0.4 for the full height of 30 cm, but is still dominated by bed drag, rendering the assumption of dense-canopy behavior for *ah>0.1* invalid. Calculation of *ah* in this case is nonetheless rather difficult as we did not use single elements of a given width, but a shoot-like structure which parts from 5-mm width near the bed (for VBD *constant* and *above*) and separates into 6 blades of 3-mm width or two blades of 25 mm for the VBD *constant* and *above,* respectively (Table 1). This means that *ah* varies with respect to *z* and exact determination of the overall dominating roughness density for each setting is not very straight forward. The differences in velocity profiles in figure 4 show the dependence on both magnitude of velocity and in-canopy distance *x* for the canopy to trigger an S-shaped curve on the profile, regardless of initial roughness density.

When focusing on the effect of VBD on velocity, the differences are clear when analyzing the profiles at B and C. In general, The VBD *below* caused the highest reduction on velocity within the canopy (see figure 5); however, it also yielded the highest velocities above the canopy. VBD *constant* yielded similar reduction capacities as the VBD *below* and caused less acceleration above the canopy. VBD *above* delivered the poorest performance displaying very little reduction for low velocities (5 and 10 cm/s) and a slight decrease for 20 and 30 cm/s. Additionally, the velocity profile after 1 m of ASG remained virtually unchanged by the VBD *below* and reduction could be seen in a more significant manner only after the second meadow (at C). Table 2 shows column-averaged values of the velocity above and within the canopy. VBD is also a factor affecting the onset of a shear layer above the canopy. This is due to the increase in velocity in the lower part of the meadow, where the least reduction in velocity takes place. Stems on vegetation whose biomass is more spatially distributed upwards will reduce less flow than the leaves above. Koch et al. (2006) describes these differences regarding VBD and the effect on the velocity profile. It is important to note, however, that the present study used a single material as surrogate, varying solely the width to represent different VBDs; therefore, biomechanical properties remain similar for all experiments. Notwithstanding, the increased width (either below or above) did play a role: the bending of the ASG with

8

each velocity varied greatly with VBD. A larger width means a larger flexural stiffness (see equation for *EI* in Fonseca & Koehl, 2006), and hence a lower bending angle (see plant positions in figure 6). Streamlining therefore occurs less in the lower area and more in the upper, and for this reason it is the greatest reduction achieved for this VBD. For VBD *above*, on the other hand, the low flexural stiffness at the bottom cause it to lean with a very low angle, very close to the bed, thus keeping velocity reduction at a minimum.

Table 2 Average difference in u_x [%] (at 20 cm/s) for canopy and above-canopy layers compared to the reference velocity.

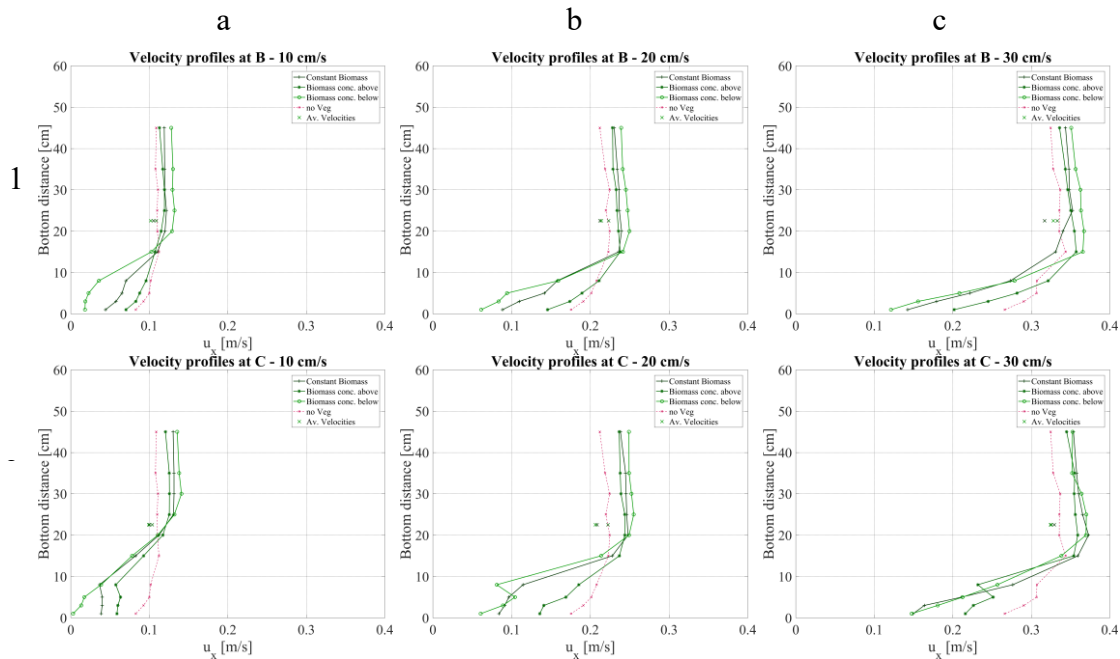|	Position	Above-canopy	Within canopy
Constant	B	9.04	-24.5
	C	13.3	-37.8
Above	B	7.28	-5.61
	C	11.2	-14.3
Below	B	13.05	-30.28
	C	16.4	-45.2

Figure 5 Comparison of velocity profiles for each VBD tested at point B (row 1) and C (row 2), after the second meadow; for velocities (a) 10 cm/s, (b) 20 cm/s and (c) 30 cm/s.

In general, all VBDs triggered a reduction in velocity which was more apparent after 2m. This shows that reduction increases with respect to *x* within each canopy. Figure 6 shows contour plots with an interpolation of the velocity field inside and above the canopy and its evolution along the study segment. The reduction in velocity is proportional to the magnitude of velocity, whereby reduction in velocity is lower with increasing distance *x* from the origin. With an experimental length greater than the one available in this study, a maximum reduction could be identified for each specific VBD and velocity. Here, it is only possible to observe such a behavior with high velocities of 30 cm/s, where it shows a horizontally layered behavior for the velocity field (fig. 6), meaning that no further change in velocity is achieved with inc-
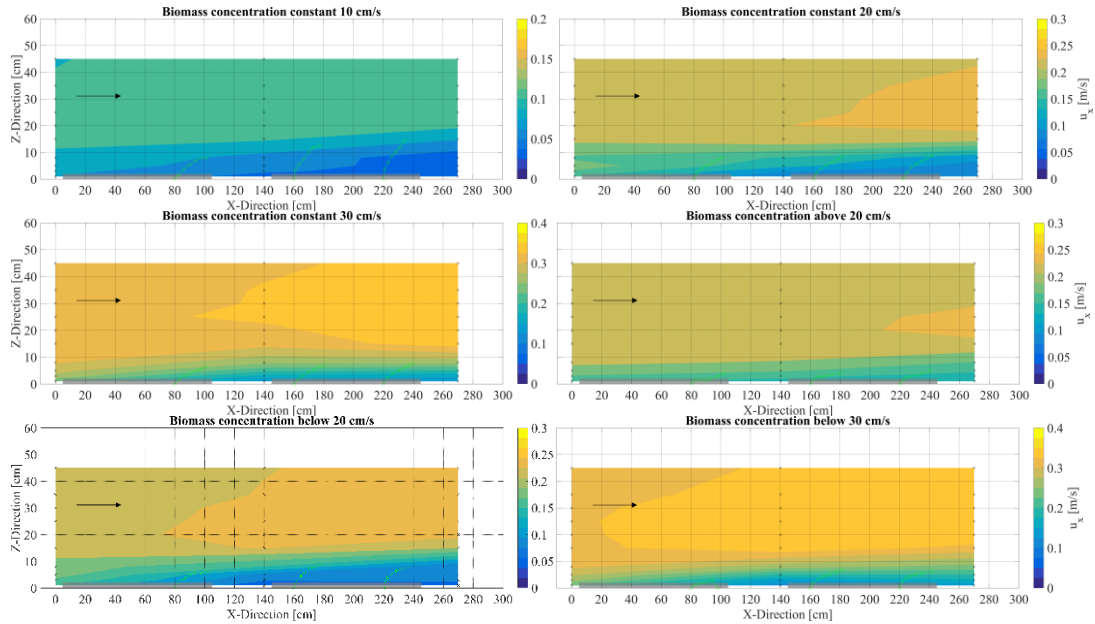
Villanueva, Paul, Vogt and Schlurmann

Figure 6 Contour plot for (left-to-right and up-to-down) *constant* VBD at 10, 20 and 30 cm/s, VBD *above* for 20 cm/s and VBD *below* for 20 and 30 cm/s.

reasing *x*.

Figure 6 also shows the position of the meadows (gray-shaded areas) and the averaged position of the plants (green solid line) for each given velocity-VBD combination. The VBD *constant* is shown at 3 velocities to use as reference; VBD *above* for 10 cm/s is similar to that of the constant VBD, and for 30 cm/s there is not much change from the velocity of 20 cm/s; finally, for the VBD *below*, 10 cm/s is also very similar to the lower velocities for the other 2 VBDs, while 20 and 30 cm/s, as shown in the figure, show higher degrees of velocity reduction. Moreover, the higher the bending angle of the blades (with respect to *y*), the lower the attenuation of velocity. As shown also in Table 2, for a current flow of 20 cm/s, the averaged velocity above the canopy increases around 9-13%, depending on the VBD, while reduction within the canopy can reach values above 30%. As is to be expected, the average velocity for the whole water column varies less than 1%, following energy balance and continuity; small variations of fractions of millimeters could be measured (not presented in this note), which are the cause of the differences between averaged velocities before and after the meadows.

CONCLUSIONS

Seagrass meadows reduce current flow and outset sedimentation (Nepf, 2012; Gambi et al., 1990; Ondiviela et al., 2014). Studying the effects of vegetation is an arduous task given difficulties to measure on field and plant sensibility towards changes in environment, making lab tests with actual plants a rather challenging endeavor. Artificial materials can therefore be utilized as mimics, but suitability must first be tested. Several studies have done this already for hydrodynamic studies (Fonseca & Koehl, 2006; Paul et al, 2012), and even for restoration and ecosystem preservation purposes (e.g. Tuya et al., 2017). This study focused specifically on the influence of seagrass (represented by polyethylene surrogates) on currents, and tested these against a unidirectional current on a circular track-flume. The effect of the artificial elements was in accordance with other flume tests, reducing current

Villanueva, Paul, Vogt and Schlurmann

significantly within the canopy. Furthermore, the tests were done with a shoot density within the low-end of what can be found in nature, this being much lower than what has been usually tested; showing that even for a low density, the effect of flexible element within the flow is significant enough to distort the velocity profile. Moreover, seagrass meadows create a lower hydrodynamic loading within the meadow, while increasing the velocity above the meadow slightly, creating a skimming flow above the canopy (Widdows et al., 2008). But this effect on current velocity is also moderated by the vertical biomass distribution, which varies completely depending on the seagrass species. The idealized experiments here – with constant shoot density and varying vertical biomass distribution – showed that this is a determining factor on the magnitude of reduction of velocity, with averaged reduction being up to threefold for a biomass concentrated on the lower part of the shoot, compared to plants with thinner and taller stems and biomass concentrated on the upper part.

On the x-direction, velocity decreased gradually as the current flowed through a longer stretch of (artificial) vegetation. Studies of the total extent of the influence in velocity are encouraged for seagrasses as add-on to this study. Furthermore, this study did not take into account the influence of the total patch width (y-direction), but used the whole width of the flume (1 m) and measured velocities in the center. In reality, however, seagrass patches are found surrounded by currents from all sides; Bouma et al. (2005), for instance, did similar flume experiments using unidirectional currents with both actual and artificial vegetation, including side currents to replicate actual conditions of tidal currents as accurately as possible; in their results, shoot stiffness plays a major role in resistance to hydrodynamic loading.

The importance of seagrasses as ecosystem engineers should not be ignored. Several studies have demonstrated the importance of vegetation regarding this aspect, but restoration attempts are still at an initial stage. Further development of this study will include sedimentation and wave attenuation, which are important factors regarding seed survival and the ability of artificial elements to provide the necessary shelter for seagrass to regrow.

REFERENCES
Bouma, T. J., De Vries, M. B., Low, E., Peralta, G., Tánczos, I. V., van de Koppel, J., & Herman, P. J. (2005). Trade-offs related to ecosystem engineering: A case study on stiffness of emerging macrophytes. *Ecology*, *86*(8), 2187-2199.,

Fonseca, M. S., & Koehl, M. A. R. (2006). Flow in seagrass canopies: the influence of patch width. *Estuarine, Coastal and Shelf Science*, *67*(1), 1-9.

Gambi, M. C., Nowell, A. R., & Jumars, P. A. (1990). Flume observations on flow dynamics in Zostera marina (eelgrass) beds. *Marine ecology progress series*, 159-169.

Ghisalberti, M., & Nepf, H. (2009). Shallow flows over a permeable medium: the hydrodynamics of submerged aquatic canopies. *Transport in porous media*, *78*(2), 309-326.

Goring, D. G., & Nikora, V. I. (2002). Despiking acoustic Doppler velocimeter data. *Journal of Hydraulic Engineering*, *128*(1), 117-126.

Goseberg, N., Wurpts, A., & Schlurmann, T. (2013). Laboratory-scale generation of tsunami and long waves. *Coastal Engineering*, *79*, 57-74.

Koch, E. W. (2001). Beyond light: physical, geological, and geochemical parameters as possible submersed aquatic vegetation habitat requirements. *Estuaries*, *24*(1), 1-17.

11

Koch, E. W., Ackerman, J. D., Verduin, J., & van Keulen, M. (2007). Fluid dynamics in seagrass ecology—from molecules to ecosystems. In *SEAGRASSES: BIOLOGY, ECOLOGYAND CONSERVATION* (pp. 193-225). Springer Netherlands.

Losada, I. J., Maza, M., & Lara, J. L. (2016). A new formulation for vegetation-induced damping under combined waves and currents. *Coastal Engineering*, *107*, 1-13.

Luhar, M., & Nepf, H. M. (2011). Flow-induced reconfiguration of buoyant and flexible aquatic vegetation. *Limnology and Oceanography*, *56*(6), 2003-2017.

Möller, I., Kudella, M., Rupprecht, F., Spencer, T., Paul, M., Van Wesenbeeck, B. K., ... & Schimmels, S. (2014). Wave attenuation over coastal salt marshes under storm surge conditions. *Nature Geoscience*, *7*(10), 727-731.

Nepf, H. M., & Vivoni, E. R. (2000). Flow structure in depth-limited, vegetated flow. *Journal of Geophysical Research: Oceans*, *105*(C12), 28547-28557.

Nepf, H. M. (2012). Flow and transport in regions with aquatic vegetation. *Annual Review of Fluid Mechanics*, *44*, 123-142.

Niklas, K. J. (1992). Plant biomechanics: an engineering approach to plant form and function. *University of Chicago press*.

Okamoto, T. A., & Nezu, I. (2009). Turbulence structure and "Monami" phenomena in flexible vegetated open-channel flows. *Journal of Hydraulic Research*, *47*(6), 798-810.

Orth, R. J., Carruthers, T. J., Dennison, W. C., Duarte, C. M., Fourqurean, J. W., Heck, K. L., ... & Short, F. T. (2006). A global crisis for seagrass ecosystems. *AIBS Bulletin*, *56*(12), 987-996.

Paul, M., Bouma, T. J., & Amos, C. L. (2012). Wave attenuation by submerged vegetation: combining the effect of organism traits and tidal current. *Marine Ecology Progress Series*, *444*, 31-41.

Paul, M., Henry, P. Y., & Thomas, R. E. (2014). Geometrical and mechanical properties of four species of northern European brown macroalgae. *Coastal engineering*, *84*, 73-80.

Paul, M., & Gillis, L. G. (2015). Let it flow: how does an underlying current affect wave propagation over a natural seagrass meadow?. *Marine Ecology Progress Series*, *523*, 57-70.

Paul, M., Rupprecht, F., Möller, I., Bouma, T. J., Spencer, T., Kudella, M., ... & Schimmels, S. (2016). Plant stiffness and biomass as drivers for drag forces under extreme wave loading: A flume study on mimics. *Coastal Engineering*, *117*, 70-78.

Peralta, G., Bouma, T. J., van Soelen, J., Pérez-Lloréns, J. L., & Hernández, I. (2003). On the use of sediment fertilization for seagrass restoration: a mesocosm study on Zostera marina L. *Aquatic Botany*, *75*(2), 95-110.

Schendel, A., Goseberg, N., & Schlurmann, T. (2015). Erosion stability of wide-graded quarry-stone material under unidirectional current. *Journal of Waterway, Port, Coastal, and Ocean Engineering,* 142(3), 04015023.

Tuya, F., Vila, F., Bergasa, O., Zarranz, M., Espino, F., & Robaina, R. R. (2017). Artificial seagrass leaves shield transplanted seagrass seedlings and increase their survivorship. *Aquatic Botany*, *136*, 31-34.

Van Katwijk, M. M., Bos, A. R., De Jonge, V. N., Hanssen, L. S. A. M., Hermus, D. C. R., & De Jong, D. J. (2009). Guidelines for seagrass restoration: importance of habitat selection and donor population, spreading of risks, and ecosystem engineering effects. *Marine pollution bulletin*, *58*(2), 179-188.

Vogel, S. (1994). *Life in moving fluids: the physical biology of flow*. Princeton University Press.

Waycott, M., Duarte, C. M., Carruthers, T. J., Orth, R. J., Dennison, W. C., Olyarnik, S., ... & Kendrick, G. A. (2009). Accelerating loss of seagrasses across the globe threatens coastal ecosystems. *Proceedings of the National Academy of Sciences*, *106*(30), 12377-12381.

Widdows, J., Pope, N. D., Brinsley, M. D., Asmus, H., & Asmus, R. M. (2008). Effects of seagrass beds (Zostera noltii and Z. marina) on near-bed hydrodynamics and sediment resuspension. *Marine Ecology Progress Series*, *358*, 125-136.

Villanueva, Paul, Vogt and Schlurmann